

Reactions of Sn(NMe₂)₂ with Alkali-Metal *tert*-Butylphosphides ^tBuPHM (M = Li, Na, K): Evidence for Metal-Induced Modification of the Tin(II) Phosphinidene Anions

Felipe García, Jörg P. Hehn, Richard A. Kowenicki, Mary McPartlin, Christopher M. Pask, Alexander Rothenberger, Matthew L. Stead, and Dominic S. Wright*

Chemistry Department, University of Cambridge, Lensfield Road, Cambridge CB2 1EW, United Kingdom

Received February 21, 2006

The 1:2 or 1:3 stoichiometric reactions of Sn(NMe₂)₂ with ^tBuPHM (M = Li, Na, K) in THF give the heterometallic alkali-metal/Sn(II) phosphinidene cages [{Sn₂(P^tBu)₃]₂Li₄·4THF} (1), [{Sn₃(P^tBu)₄]₂Na·3THF} [Na(THF)₆]⁺ (2), [{Sn₃(P^tBu)₄]₂(K·THF)₃} [K(THF)₆]⁺ (4), and [{Sn₄(P^tBu)₅]₂K₂·5THF} (5) (THF = C₄H₈O). The 2:3 → 3:4 → 4:5 numerical progression observed in the Sn(II):P^tBu ratios of the [{Sn₂(P^tBu)₃]₂]⁴⁻, [{Sn₃(P^tBu)₄]₂]²⁻, and [{Sn₄(P^tBu)₅]₂]²⁻ anions of these complexes is dependent on the alkali-metal counteranions present. The fact that the Lewis base donor has no effect on the resulting Sn(II) phosphinidene anions is indicated by the formation of the PMDETA-solvated complex [{Sn₃(P^tBu)₄]₂Na₂·2PMDETA·THF} (3) (PMDETA = (Me₂NCH₂CH₂)₂NMe) in the 1:2 reaction of Sn(NMe₂)₂ with ^tBuPHNa in the presence of PMDETA (containing the same [{Sn₃(P^tBu)₄]₂]²⁻ dianion as found in 2). The syntheses and X-ray structures of the new complexes 2–5 are discussed in relation to those of the previously reported complex 1.

Introduction

Our interest in main-group-metal phosphinidene compounds stems from their potential applications in the low-temperature deposition of a large range of alloys from solution.¹ We found, for example, that the Sb(III)/Li cage [{Sb(PCy)₃]₂Li₆·6Me₂NH]² is valuable in the deposition of photoactive Sb/Li films,^{1b} decomposing at 30–40 °C from solution initially into the Zintl compound [Sb₇Li₃·6Me₂NH], which loses Me₂NH upon exposure to a vacuum to give the alloy. The driving force for this type of “cage-to-alloy” reaction is the formation of thermodynamically stable P–P single bonds, which have the greatest homoatomic bond energies of any of the group 15 elements.³ Recent studies of Sn(II) phosphinidene compounds have allowed a more detailed understanding of the mechanism of formation of metal–metal bonds via reductive elimination and, in particular, the important influence of alkali-metal cations on the extent of the reactions.⁴ In particular, the observed greater formation of P–P and metal–metal bonds in the products formed as the size of the alkali-metal cation increases appears to be a direct consequence of the greater nucleophilicity and basicity of the P–alkali-metal bonds. This is seen in particular in the outcomes of the reactions of Sn(NMe₂)₂ with CyPHM (Cy = cyclohexyl; M = Li, Na, K) in THF. For M = Li, the macrocyclic tetraanion [{Sn(μ-PCy)₂(μ-PCy)]₂]⁴⁻ is obtained (Figure 1a), whereas one of the major products of the reaction

involving M = Na is the [{Sn₂(μ-PCy)₂(PCy-PCy)]₂]²⁻ dianion (Figure 1b).⁵ Moving to M = K, the dianion [Sn₂(μ-PCy-PCy)₂]²⁻ (μ-PCy)₂]²⁻ is isolated (Figure 1c).⁵ These anions result from successive CyP insertion reactions into the Sn(II) phosphinidene frameworks: e.g., Scheme 1.

We present here a study of the reactions of ^tBuPHM (M = Li, Na, K) with Sn(NMe₂)₂. Unlike analogous reactions involving the less sterically demanding Cy group,⁵ no P–P or Sn–Sn bond formation is observed within the series of heterometallic cages produced. Thus, the direct effects of the size of the alkali-metal cations alone on the resulting phosphinidene cages generated can be gauged for the first time in these systems (i.e., without the complication of side reactions). We report the syntheses and structures of the new complexes [{Sn₃(P^tBu)₄]₂Na·3THF} [Na(THF)₆]⁺ (2), [{Sn₃(P^tBu)₄]₂Na₂·2PMDETA·THF} (3), [{Sn₃(P^tBu)₄]₂(K·THF)₃} [K(THF)₆]⁺ (4), and [{Sn₄(P^tBu)₅]₂K₂·5THF} (5). Comparison of the structures of these complexes with the Li complex [{Sn(μ-P^tBu)]₂(μ-P^tBu)]₂(Li·THF)₄ (1), which we have mentioned in a previous communication,⁶ reveals a change in the Sn(II) phosphinidene anion from a metallacyclic [{Sn(μ-P^tBu)]₂(μ-P^tBu)]₂]⁴⁻ unit in 1 to a tripodal arrangement of the [Sn₃(P^tBu)₄]₂]²⁻ dianion in 2–4. In 5 (obtained as a minor product along with 4) a further modification of the phosphinidene unit is observed, presumably in response to the presence of a larger alkali metal.

Results and Discussion

In a previous communication we had reported briefly that the 1:3 reaction of Sn(NMe₂)₂ with ^tBuPHLi in THF gives the heterometallic Sn(II)/Li cage [{Sn₂(P^tBu)₃]₂Li₄·4THF} (1; in 38% yield),⁶ composed of a [{Sn(μ-P^tBu)]₂(μ-P^tBu)]₂]⁴⁻ tet-

* To whom correspondence should be addressed. E-mail: dsw1000@cus.cam.ac.uk. Fax: 0044 (0)1223 336362.

(1) (a) Hopkins, A. D.; Woods, J. A.; Wright, D. S. *Coord. Chem. Rev.* **2001**, *216*, 155. (b) Beswick, M. A.; Harmer, C. N.; Hopkins, A. D.; McPartlin, M.; Wright, D. S. *Science* **1998**, *281*, 1500.

(2) Beswick, M. A.; Goodman, J. M.; Harmer, C. N.; Hopkins, A. D.; Paver, M. A.; Raithby, P. R.; Wheatley, A. E. H.; Wright, D. S. *J. Chem. Soc., Chem. Commun.* **1997**, 1897.

(3) Huheey, J. E.; Keiter, E. A.; Keiter, R. L. *Inorganic Chemistry, Principles of Structure and Reactivity*, 4th ed.; Harper and Row: New York, 1993, and references therein.

(4) García, F.; Hopkins, A. D.; Pask, C. M.; Woods, A. D.; Wright, D. S. *J. Mater. Chem.* **2004**, 3093.

(5) Alvarez, P.; Bond, A. D.; Lawson, G. T.; McPartlin, M.; Woods, A. D.; Wright, D. S. Unpublished results.

(6) Davies, J. E.; Hopkins, A. D.; Rothenberger, A.; Woods, A. D.; Wright, D. S. *Chem. Commun.* **2001**, 525.

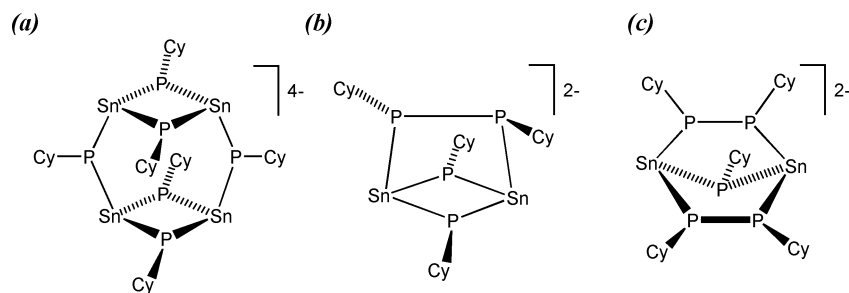
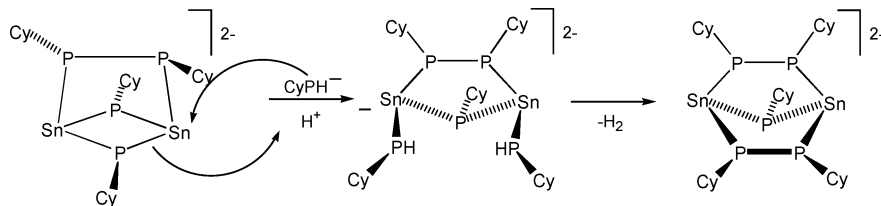


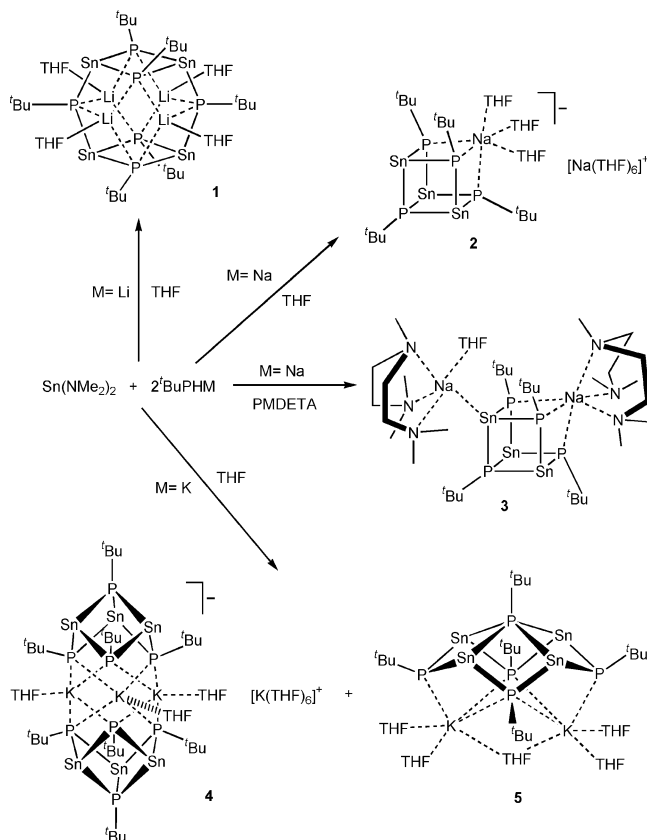
Figure 1. Structures of the anions (a) $[\{\text{Sn}(\mu\text{-PCy})\}_2(\mu\text{-PCy})]_2^{4-}$, (b) $[\{\text{Sn}_2(\mu\text{-PCy})_2(\text{PCy-PCy})\}]_2^{2-}$, and (c) $[\text{Sn}_2(\mu\text{-PCy-PCy})_2(\mu\text{-PCy})]_2^{2-}$.

Scheme 1. Insertion of a CyP Unit into the Framework of the $[\{\text{Sn}(\mu\text{-PCy})\}_2(\text{CyP-PCy})]_2^{2-}$ Dianion, Generating $[\text{Sn}_2(\mu\text{-PCy-PCy})_2(\mu\text{-PCy})]_2^{2-}$



raanion (similar to that shown in Figure 1a) which coordinates four Li^+ cations within the cavity of the macrocycle (Scheme 2). Since no experimental data on **1** were reported in our previous communication,⁶ full details of the synthesis and characterization of this complex have been included here. As noted in the Introduction, in the reactions of CyPHM ($M = \text{Li}, \text{Na}, \text{K}$) with $\text{Sn}(\text{NMe}_2)_2$ the effect of changing from Li to the heavier alkali metals (Na, K) is to encourage P–P bond formation.⁵ We wondered what the result of changing the alkali metal in analogous reactions of the more sterically demanding $t\text{BuPHM}$ would be on the nature of the products isolated. Accordingly, the reactions of $\text{Sn}(\text{NMe}_2)_2$ with $t\text{BuPHM}$ ($M = \text{Na}, \text{K}$) in THF were investigated. A 1:2 stoichiometric reaction involving $t\text{BuPHNa}$ produces $[\{\text{Sn}_3(\text{P}^t\text{Bu})_4\}\text{Na}\cdot 3\text{THF}]^- [\text{Na}(\text{THF})_6]^+$ (**2**), while a reaction involving $t\text{BuPHK}$ gives $[\{\text{Sn}_3(\text{P}^t\text{Bu})_4\}_2(\text{K}\cdot\text{THF})_3]^- [\text{K}(\text{THF})_6]^+$ (**4**) which is normally contaminated by a small amount of $[\{\text{Sn}_4(\text{P}^t\text{Bu})_5\}\text{K}_2\cdot 5\text{THF}]$ (**5**) (Scheme 2). Complexes **2** and **4** contain the $[\{\text{Sn}_3(\text{P}^t\text{Bu})_4\}]_2^{2-}$ dianion, whereas **5** contains the $[\{\text{Sn}_4(\text{P}^t\text{Bu})_5\}]_2^{2-}$ dianion (Figure 2a,b, respectively). The elemental analysis of **4** was complicated by the presence of **5** as an impurity and (like **2**) by the lability of the THF ligands, which are partially removed by placing the complex under vacuum during isolation. To assess the effect(s) of the Lewis base donor present, the reaction of $t\text{BuPHNa}$ in THF in the presence of the tridentate Lewis base donor PMDETA ($=(\text{Me}_2\text{NCH}_2\text{CH}_2)\text{NMe}_2$) was also carried out. The product is $[\{\text{Sn}_3(\text{P}^t\text{Bu})_4\}\text{Na}_2\cdot 2\text{PMDETA}\cdot\text{THF}]$ (**3**), having exactly the same $[\{\text{Sn}_3(\text{P}^t\text{Bu})_4\}]_2^{2-}$ anion as that found in the Na^+ complexes **2** and **4**. This result indicates that the Lewis base present has no bearing on the Sn(II) phosphinidene framework formed. Unlike **2**, in which the THF ligands are labile and can be partially removed by placing the complex under vacuum, the chelate PMDETA ligands of **3** are robust under these conditions and no problems were encountered obtaining satisfactory elemental analysis. Westerhausen and co-workers have previously reported the structure of the Ba^{2+} complex $[\{\text{Sn}_3(\text{PSi}^t\text{Bu}_3)_4\}\text{Ba}\cdot\eta^6\text{-C}_6\text{H}_5\text{CH}_3]$, containing a $[\{\text{Sn}_3(\text{PSi}^t\text{Bu}_3)_4\}]_2^{2-}$ dianion which is similar to that present in **2–4**,⁷ which is obtained from the reduction of the Sn(II) cubane

Scheme 2



$[\text{Sn}\{\mu_3\text{-P}(\text{Si}^t\text{Bu}_3)\}_4]$ with distilled Ba metal. However, to our knowledge the $[\{\text{Sn}_4(\text{P}^t\text{Bu})_5\}]_2^{2-}$ anion of **5** (Figure 2c) is a completely novel Sn(II) phosphinidene arrangement.

The presence of volatile THF ligands in **1–5** and/or their extreme air sensitivity made elemental and spectroscopic analysis of the complexes difficult. Elemental analysis of **2** showed that after placing the complex under vacuum during isolation approximately six THF ligands are lost. The loss of THF ligands is also apparent in the case of **4/5**, where approximately four THF ligands are displaced when the solid complex is placed under vacuum during isolation. To avoid

(7) Westerhausen, M.; Krofta, M.; Wiberg, N.; Knizek, J.; Nöth, H.; Pfitzner, A. *Z. Naturforsch.* **1998**, *53b*, 1489. Westerhausen, M.; Krofta, M.; Schneiderbauer, P.; Piotrowski, H. *Z. Anorg. Allg. Chem.* **2005**, *631*, 1391.

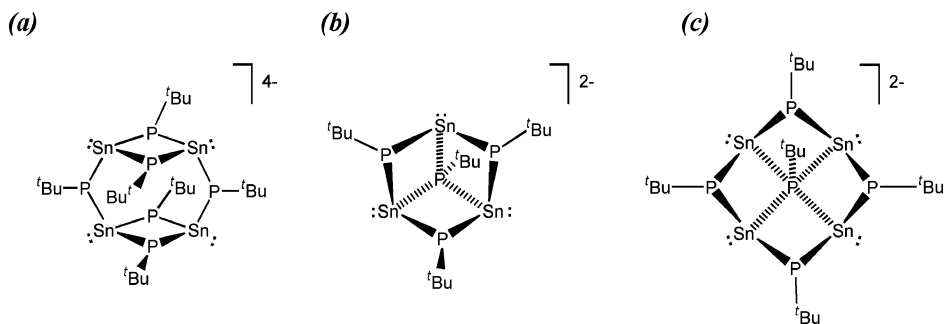


Figure 2. Structures of (a) the $[\{\text{Sn}(\mu\text{-P}^t\text{Bu})\}_2(\mu\text{-P}^t\text{Bu})]^{4-}$ anion of **1**, (b) the $[\{\text{Sn}_3(\text{P}^t\text{Bu})_4\}]^{2-}$ anion of **2–4**, and (c) the $[\{\text{Sn}_4(\text{P}^t\text{Bu})_5\}]^{2-}$ anion of **5**.

Table 1. Crystal and Structure Solution Data for $[\{\text{Sn}_2(\text{P}^t\text{Bu})_3\}_2\text{Li}_4\cdot 4\text{THF}]$ (1**), $[\{\text{Sn}_3(\text{P}^t\text{Bu})_4\}\text{Na}\cdot 3\text{THF}][\text{Na}(\text{THF})_6]^+$ (**2**), $[\{\text{Sn}_3(\text{P}^t\text{Bu})_4\}\text{Na}_2\cdot 2\text{PMDETA}\cdot \text{THF}\cdot 0.5(\text{hexane})]$ (**3}\cdot 0.5(\text{hexane})**), $[\{\text{Sn}_3(\text{P}^t\text{Bu})_4\}_2(\text{K}\cdot \text{THF})_3][\text{K}(\text{THF})_6]^+\cdot \text{THF}$ (**4}\cdot \text{THF}**), and $[\{\text{Sn}_4(\text{P}^t\text{Bu})_5\}\text{K}_2\cdot 5\text{THF}\cdot 2\text{THF}]$ (**5}\cdot 2\text{THF}**)^a**

	1	2	3}\cdot 0.5(\text{hexane})	4}\cdot \text{THF}	5}\cdot 2\text{THF}
empirical formula	C ₄₀ H ₈₆ Li ₄ O ₄ - P ₆ Sn ₄	C ₅₂ H ₁₀₈ Na ₂ O ₉ - P ₄ Sn ₃	C ₄₁ H ₉₄ N ₆ Na ₂ O- P ₄ Sn ₃	C ₇₂ H ₁₅₂ K ₄ O ₁₀ - P ₈ Sn ₆	C ₄₈ H ₁₀₁ K ₂ O ₇ - P ₅ Sn ₄
fw	1319.57	1403.31	1213.15	2294.24	1498.10
cryst syst	monoclinic	rhombohedral	monoclinic	orthorhombic	monoclinic
space group	<i>P</i> 2 ₁ / <i>n</i>	<i>R</i> 3	<i>P</i> 2 ₁ / <i>c</i>	<i>P</i> 2 ₁ 2 ₁ 2 ₁	<i>P</i> 2 ₁ / <i>m</i>
<i>a</i> /Å	13.4566(5)	15.723(2)	12.883(3)	19.189(4)	12.085(2)
<i>b</i> /Å	15.1203(6)	15.723(2)	17.341(4)	20.450(4)	18.656(4)
<i>c</i> /Å	14.7018(5)	26.341(5)	28.301(6)	28.608(6)	15.417(3)
β /deg	92.074(2)		92.83(3)		103.02(3)
<i>V</i> /Å ³	2989.38(19)	5639.7(16)	6315(2)	11226(4)	3386.4(12)
<i>Z</i>	2	3	4	4	2
<i>F</i> (000)	1320	2172	2489	4640	1516
θ range (deg)	3.55–27.53	4.03–25.00	3.52–27.46	3.55–26.02	3.53–25.00
cryst size (mm)	0.18 × 0.12 × 0.12	0.16 × 0.16 × 0.10	0.15 × 0.15 × 0.10	0.46 × 0.16 × 0.12	0.16 × 0.13 × 0.12
ρ_{calcd} (Mg m ⁻³)	1.466	1.240	1.276	1.357	1.469
μ (Mo K α)/mm ⁻¹	1.843	1.126	1.323	1.617	1.738
no. of rflns collected	19 754	13 165	26 243	46 996	18 152
no. of indep rflns (<i>R</i> _{int})	6828 (0.043)	3938 (0.033)	11 344 (0.085)	19 979 (0.045)	6070 (0.049)
abs cor	"multiscan"	"multiscan"	"multiscan"	"multiscan"	"multiscan"
max, min transmissn	0.806, 0.774	0.894, 0.821	0.873, 0.652	0.687, 0.830	0.844, 0.719
no. of data/restraints/params	6828/96/231	3938/77/191	5351/14/503	19 979/0/898	6070/150/310
goodness of fit on <i>F</i> ²	1.029	0.927	1.042	1.014	1.073
<i>R</i> values (<i>I</i> > 2 σ <i>I</i>)					
<i>R</i> 1	0.050	0.051	0.056	0.045	0.062
w <i>R</i> 2	0.119	0.134	0.142	0.102	0.147
<i>R</i> values (all data)					
<i>R</i> 1	0.077	0.059	0.098	0.067	0.085
w <i>R</i> 2	0.134	0.141	0.165	0.116	0.155
peak and hole/e Å ⁻³	0.712, -0.858	0.157, -0.227	0.838, -0.603	0.538, -0.490	1.900, -0.659
abs structure param		0.01(5)		0.01(2)	

^a For all compounds, *T*/*K* = 180(2) and $\lambda = 0.710\ 73\ \text{Å}$.

extensive hydrolysis in solution, NMR solvents had to be degassed (by freeze/thaw techniques) and dried with a sodium mirror. The ¹H NMR spectra for all the complexes (in arene solvents) were as expected, showing the presence of ^tBu groups as singlets at ca. δ 1.5–2.2, together with the expected resonances for the Lewis base ligands (THF or PMDETA). The room-temperature ³¹P NMR spectrum of **1** (in toluene) shows two broad multiplets (δ -184.9 and -250.0) for the μ -P^tBu within and linking the Sn₂P₂ dimer units of the metallacyclic $[\{\text{Sn}(\mu\text{-P}^t\text{Bu})\}_2(\mu\text{-P}^t\text{Bu})]^{4-}$ tetraanion (presumably resulting from unresolved ³¹P-⁷Li coupling). The appearance of this spectrum is very similar to that found for the isostructural complex $[\{\text{Sn}(\mu\text{-PCy})\}_2(\mu\text{-PCy})_2](\text{Li}\cdot\text{THF})_4$, which also exhibits two multiplets in its ³¹P NMR spectrum at room temperature (δ -184.5 and -249.5).⁶ The room-temperature ³¹P NMR spectra of **2** and **3** (in THF) show two broad singlets in a ca. 1:3 ratio (δ -145.2 and -175.9 in **2**; δ -142.7 and -179.4 in **3**) (with broad ^{119/117}Sn satellites also present), corresponding to the two P environments within their *intact* [Sn₃(P^tBu)₄]²⁻ anions. In **2**, a minor Sn(II) solution species at δ -156.8 is also present. In **4/5**, four broad resonances were found in THF solution at room temperature (δ -123.2 (s), -135.2 (s), -143.0

(s), -153.3 (s) (major)). The ¹¹⁹Sn spectra of **2** and **3** (in THF) exhibit a pseudo-quartet at ca. δ 800, which can be assigned to the *intact* [Sn₃(P^tBu)₄]²⁻ units of the complexes, resulting presumably from the coupling constants for the two P environments bonded to each Sn center being almost identical. Minor solution species are also present in the ¹¹⁹Sn NMR spectra of **2** and **3** at δ 830.0 and 757.3, respectively. In the related [Sn₃(PSi^tBu₃)₄]²⁻ dianion, the ³¹P NMR spectrum is that of a doublet (δ -246.8) and a triplet (δ 528.6), and the ¹¹⁹Sn NMR spectrum appears as the expected doublet of triplets (δ 744) (which collapses to a pseudo-quartet in **2** and **3**).^{7a} Despite using a saturated solution of **4/5** (>50 mg/0.7 mL in THF), only a very broad singlet could be observed in the ¹¹⁹Sn NMR spectrum at room temperature (δ 846.0, *w*_{1/2} = ca. 2500 Hz). This resonance is possibly the unresolved quartet of the [Sn₃(P^tBu)₄]²⁻ anion of the major component **4**.

The low-temperature X-ray structures of **1–5** were obtained. Details of the data collections and structure solutions are shown in Table 1. Selected bond lengths and angles for these complexes are shown in Tables 2–6, respectively. It should be noted that crystals of **3–5** were obtained as their hexane or THF solvates: **3}\cdot 0.5(\text{hexane})**, **4}\cdot \text{THF}**, and **5}\cdot 2\text{THF}**.

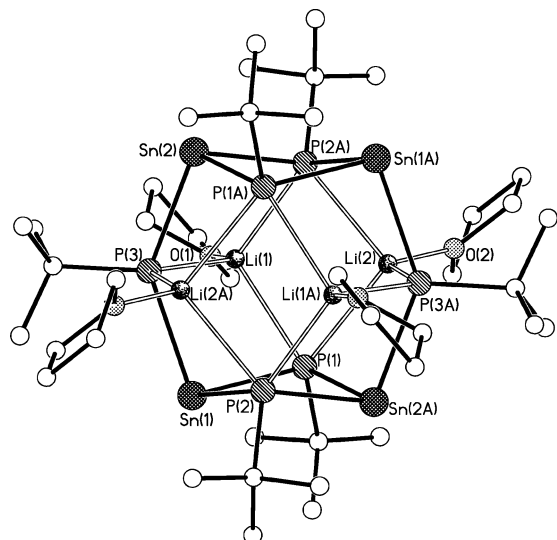


Figure 3. Centrosymmetric molecular structure of $[\{\text{Sn}_2(\text{P}^t\text{Bu})_3\}_2\text{Li}_4 \cdot 4\text{THF}]$ (**1**).

The low-temperature X-ray structure of **1** shows it to be the heterometallic complex $[\{\text{Sn}_2(\text{P}^t\text{Bu})_3\}_2\text{Li}_4 \cdot 4\text{THF}]$ (**1**) (Figure 3), containing a 14-membered $[\text{Sn}_4\text{P}_6\text{Li}_4]$ core like that found in the closely related complex $[\text{Sn}(\mu\text{-PCy})_2(\mu\text{-PCy})_2(\text{Li} \cdot \text{THF})_4]$.^{8,9} Molecules of both complexes are constructed from the association of $[\{\text{Sn}(\mu\text{-P}^t\text{Bu})\}_2(\mu\text{-P}^t\text{Bu})]_2^{4-}$ tetraanions with four THF-solvated Li^+ cations. The tetraanion unit is constructed from two $[\text{Sn}(\mu\text{-P}^t\text{Bu})_2]$ dimer rings linked together by P^tBu groups. The Sn–P bonds in **1** (range 2.588(2)–2.633(2) Å) are similar to those found in $[\{\text{Sn}(\mu\text{-PCy})\}_2(\mu\text{-PCy})_2(\text{Li} \cdot \text{THF})_4]$ (range 2.606(4)–2.628(3) Å),⁸ as are the P–Sn–P angles (range 88.14(5)–97.98(5)° in **1** and 88.4(1)–100.1(1)° in $[\{\text{Sn}(\mu\text{-PCy})\}_2(\mu\text{-PCy})_2(\text{Li} \cdot \text{THF})_4]$).⁸ The four Li^+ cations in **1** are bound to the P centers of $[\text{Sn}(\mu\text{-P}^t\text{Bu})_2]$ and to the dimer-bridging P centers. The pseudo-tetrahedral geometry of the Li^+ cations is completed by the coordination of THF ligands. The P–Li¹⁰ and P–Sn^{5–9,11} bond lengths in **1** are similar to those reported previously in a range of P–Li- and P–Sn-bonded compounds.¹² The X-ray crystallographic studies of the Na^+ complexes $[\{\text{Sn}_3(\text{P}^t\text{Bu})_4\}\text{Na} \cdot 3\text{THF}]^- [\text{Na}(\text{THF})_6]^+$ (**2**) (Figure 4) and $[\{\text{Sn}_3(\text{P}^t\text{Bu})_4\}\text{Na}_2 \cdot 2\text{PMDETA} \cdot \text{THF}]$ (**3**) (Figure 5) show that both contain the $[\text{Sn}_3(\text{P}^t\text{Bu})_4]^{2-}$ dianion. These anions function as tripodal ligands using three of the P centers to coordinate a single Na^+ cation within $\text{Sn}_3\text{P}_4\text{Na}$ cubane units in **2** and **3**. In the case of **2**, an ion-separated structure is produced in which the coordination environment of the Na^+ cation within the cubane unit is completed by bonding to three THF ligands, while the other Na^+ counterion is present within a $[\text{Na}(\text{THF})_6]^+$ complex cation. In contrast, in **3** an ion-paired arrangement is formed in which the Na^+ cation within the cubane unit is

(8) Allan, R. E.; Beswick, M. A.; Cromhout, N. L.; Paver, M. A.; Raithby, P. R.; Steiner, A.; Trevithick, M.; Wright, D. S. *J. Chem. Soc., Chem. Commun.* **1996**, 1501.

(9) See also: Nikolova, D.; von Hänisch, C.; Adolf, A. *Eur. J. Inorg. Chem.* **2004**, 2331.

(10) For examples, see: Beswick, M. A.; Wright, D. S. *Alkali Metals. Comprehensive Organometallic Chemistry II*; Pergamon: Oxford, U.K., 1995; Vol. 1, Chapter 1.

(11) For further examples, see: Westerhausen, M.; Schwarz, W. Z. *Anorg. Allg. Chem.* **1996**, 622, 903. Driess, M.; Martin, S.; Merz, K.; Pintchouk, V.; Pritzkow, H.; Grützmaier, H.; Kaupp, M. *Angew. Chem., Int. Ed.* **1997**, 36, 1894.

(12) Cambridge Structural Data Base for Visualizing Crystal Structures (January 2006): Bruno, I. J.; Cole, J. C.; Edgington, P. R.; Kessler, M.; Macrae, C. F.; McCabe, P.; Pearson, J.; Taylor, R. *Acta Crystallogr.* **2001**, b58, 389.

Table 2. Selected Bond Lengths and Angles for $[\{\text{Sn}_2(\text{P}^t\text{Bu})_3\}_2\text{Li}_4 \cdot 4\text{THF}]$ (**1**)

Bond Lengths (Å)			
Sn(1)–P(1)	2.627(2)	P(1)–Li(1)	2.615(10)
Sn(1)–P(2)	2.633(2)	P(2A)–Li(1)	2.618(11)
Sn(1)–P(3)	2.600(2)	P(3)–Li(1)	2.597(10)
Sn(2)–P(1A)	2.618(2)	P(1)–Li(2)	2.615(9)
Sn(2)–P(2A)	2.605(1)	P(2A)–Li(2)	2.587(9)
Sn(2)–P(3)	2.588(2)	P(3A)–Li(2)	2.675(10)
Bond Angles (deg)			
P(3)–Sn(1)–P(1)	94.12(5)	P(3)–Sn(2)–P(2A)	94.35(5)
P(3)–Sn(1)–P(2)	97.85(5)	P(3)–Sn(1)–P(1A)	97.98(5)
P(1)–Sn(1)–P(2)	88.14(5)		

Symmetry transformations used to generate equivalent atoms A, $-x+1$, $-y+1$, $-z+2$.

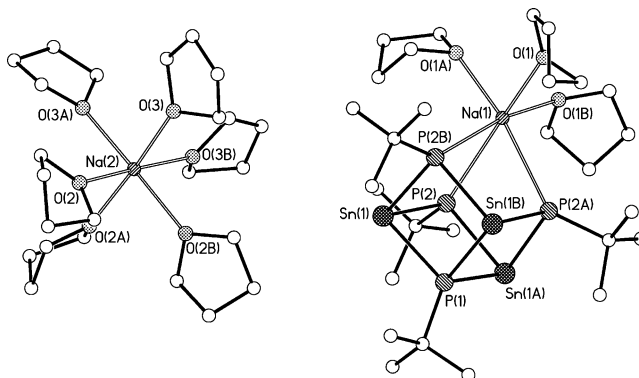


Figure 4. Structure of the ion-separated complex of $[\{\text{Sn}_3(\text{P}^t\text{Bu})_4\}\text{Na} \cdot 3\text{THF}]^- [\text{Na}(\text{THF})_6]^+$ (**2**). There is a C_3 axis through $\text{Na}(1) \cdots \text{P}(1)$ and a second parallel C_3 axis through $\text{Na}(2)$.

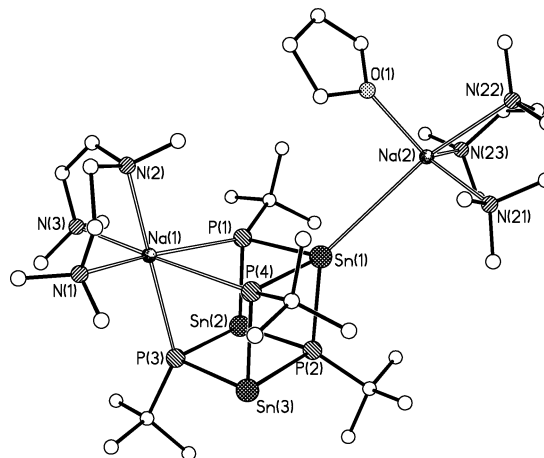


Figure 5. Structure of the ion-paired complex $[\{\text{Sn}_3(\text{P}^t\text{Bu})_4\}\text{Na}_2 \cdot 2\text{PMDETA} \cdot \text{THF}]$ (**3**).

rendered six-coordinate by solvation by PMDETA, while the other PMDETA/THF-solvated Na^+ cation is bonded to one of the Sn(II) atoms of the cubane unit. The range of Sn(II)–P^{5–9,11} and P–Na¹³ bond lengths in both complexes, and the P–Sn–P and Sn–P–Sn angles within their $\text{Sn}_3\text{P}_4\text{Na}$ cubane units, are very similar to each other and are typical of previous P–Sn- and P–Na-bonded compounds.¹² The acute P–Sn–P angles (84.15(6)–88.17(9)° in **2**; 83.28(8)–89.24(8)° in **3**) are symptomatic of the presence of a stereochemically active lone pair on each of the Sn(II) centers. In **3**, the lone pair of electrons on

(13) See for example: Andnanarison, M.; Stalke, D.; Klingebiel, U. *Chem. Ber.* **1990**, 71, 123. Koutsantonis, G. A.; Andrews, P. C.; Raston, C. L. *J. Chem. Soc., Chem. Commun.* **1995**, 47. Kuhl, O.; Sieler, J.; Baum, G.; Hey-Hawkins, E. *Z. Anorg. Allg. Chem.* **2000**, 625, 605.

Table 3. Selected Bond Lengths and Angles for $[\{\text{Sn}_3(\text{P}^i\text{Bu})_4\}\text{Na}\cdot 3\text{THF}][\text{Na}(\text{THF})_6]^+$ (2**)^a**

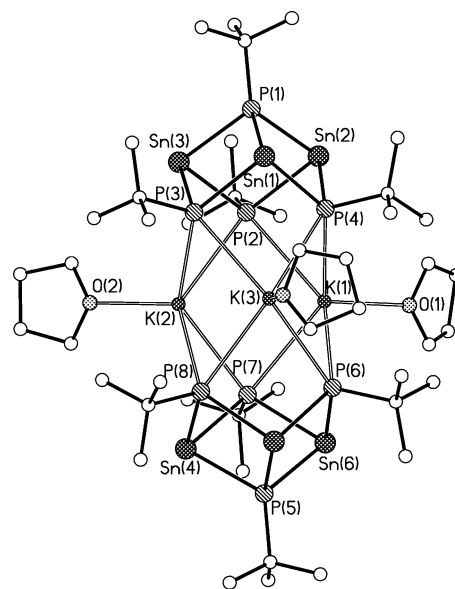
Bond Lengths (Å)			
Sn(1)–P(1)	2.615(2)	P(2)–Na(1)	3.057(5)
Sn(1)–P(2)	2.601(2)	Na(1)–O	2.364(8)
Sn(1)–P(2B)	2.607(2)	Na(2)–O (mean)	2.383(7)
P(2)–Sn(1A)	2.607(2)		
Bond Angles (deg)			
P(2)–Sn(1)–P(2B)	88.13(8)	Sn(1A)–P(1)–Sn(1)	95.31(9)
P(2)–Sn(1)–P(1)	84.38(6)	Sn(1)–P(2)–Sn(1A)	95.83(7)
P(2B)–Sn(1)–P(1)	84.25(6)	Sn(1)–P(2)–Na(1)	98.63(8)
		Sn(1A)–P(2)–Na(1)	98.48(8)

^a Symmetry transformations used to generate equivalent atoms: (A) $-y, -x + y + 1, z$; (B) $-x + y - 2, -x - 1, z$.

Table 4. Selected Bond Lengths and Angles for $[\{\text{Sn}_3(\text{P}^i\text{Bu})_4\}\text{Na}_2\cdot 2\text{PMDETA}\cdot \text{THF}]$ (3**)**

Bond Lengths (Å)			
Sn(1)–P(1)	2.598(2)	Sn(3)–P(3)	2.601(2)
Sn(1)–P(4)	2.607(2)	Sn(3)–P(4)	2.608(2)
Sn(1)–P(2)	2.609(2)	Sn(3)–P(2)	2.616(2)
Sn(1)–Na(2)	3.709(2)	P–Na(1)	2.962(4)–3.073(5)
Sn(2)–P(3)	2.591(2)	Na(2)–N	2.457(6)–2.565(6)
Sn(2)–P(1)	2.602(2)	Na(1)–N	2.26(2)–2.73(1)
Sn(2)–P(2)	2.629(2)		
Bond Angles (deg)			
P–Sn–P	83.29(5)–89.23(5)	P–Na(2)–P	72.00(7)–74.31(7)
Sn–P–Sn	93.57(9)–96.43(8)	Sn–P–Na(2)	95.51(7)–100.07(7)

Sn(1) is involved in the interaction with one of the Na⁺ cations. The Sn–Na bond in **3** (Sn(1)–Na(1) = 3.703(4) Å) is similar to those found in the few Sn–Na-bonded compounds reported previously.¹⁴ The structures of **2** and **3** are similar to that of $[\{\text{Sn}_3(\text{PSi}^i\text{Bu}_3)_4\}\text{Ba}\cdot \eta^6\text{-C}_6\text{H}_5\text{CH}_3]$, which also contains a $[\text{Sn}_3(\text{PR})_4]^{2-}$ dianion.⁷ The latter also possesses a cubane arrangement, in which the dianion acts as a tripodal ligand to the Ba²⁺ dication using three of the P centers (in a manner similar to the coordination of the Na⁺ cation within the cubane units of **2** and **3**). Unit cell analysis of several batches of crystals obtained from the reaction of Sn(NMe₂)₂ with ^tBuPHK in THF showed that the major product is $[\{\text{Sn}_3(\text{P}^i\text{Bu})_4\}_2(\text{K}\cdot\text{THF})_3][\text{K}(\text{THF})_6]^+$ (**4**) (yellow needles). However, **4** is normally contaminated by a minor amount of $[\{\text{Sn}_4(\text{P}^i\text{Bu})_5\}\text{K}_2\cdot 5\text{THF}]$ (**5**; deep orange hexagonal crystals, no more than ca. 5%). It can be noted that only $[\{\text{Sn}_3(\text{P}^i\text{Bu})_4\}\text{Na}\cdot 3\text{THF}][\text{Na}(\text{THF})_6]^+$ (**2**) was identified by a unit cell determination of samples of crystals obtained from the reaction of Sn(NMe₂)₂ with ^tBuPHNa in THF, so that the formation of the $[\text{Sn}_4(\text{P}^i\text{Bu})_5]^-$ anion of **5** appears to be unique to potassium. In the structure of $[\{\text{Sn}_3(\text{P}^i\text{Bu})_4\}_2(\text{K}\cdot\text{THF})_3][\text{K}(\text{THF})_6]^+$ (**4**), two crystallographically independent $[\text{Sn}_3(\text{P}^i\text{Bu})_4]^{2-}$ dianions coordinate three K⁺ cations within a $[\{\text{Sn}_3(\text{P}^i\text{Bu})_4\}_2(\text{K}\cdot\text{THF})_3]^-$ anion (Figure 6). The bond lengths and angles within the $[\text{Sn}_3(\text{P}^i\text{Bu})_4]^{2-}$ dianions of **4** are very similar to those found in **2** and **3** (e.g., Sn–P range 2.588(2)–2.623(3) Å, P–Sn–P range 83.99(6)–90.73(6)°; cf. 2.591(2)–2.629(2) Å, P–Sn–P range 83.29(5)–89.23(8)° in **2** and **3**). The K⁺ cations of the anion have distorted-square-based-pyramidal geometries, each being coordinated by two P centers of each of the $[\text{Sn}_3(\text{P}^i\text{Bu})_4]^{2-}$ dianions (P–K range 3.311(2)–3.391(2) Å) and by a THF ligand (K–O mean 2.664(6) Å). The range of the P–K¹⁵ bond lengths is typical of those reported previously in the literature.¹² The coordination mode

**Figure 6.** Structure of the anion in the ion-separated complex $[\{\text{Sn}_3(\text{P}^i\text{Bu})_4\}_2(\text{K}\cdot\text{THF})_3][\text{K}(\text{THF})_6]^+$ (**4**).

of the $[\text{Sn}_3(\text{P}^i\text{Bu})_4]^{2-}$ dianions in **4** is similar to that found for the group 15 anions $[\text{Sb}(\text{NCy})_3]^-$ in the neutral heterometallic complex $[\{\text{Sb}(\text{NCy})_3\}_2\text{Pb}_3]$,¹⁶ in which the three Pb^{II} centers are coordinated by two N atoms from both of the $[\text{Sb}(\text{NCy})_3]^-$ anions at the equator of the cage (resulting in a square-based-pyramidal geometry for the Pb^{II} centers, in which the fifth (exo) position is occupied by the metal lone pair). Although there is clearly no K–K bonding occurring between the positively charged K⁺ ions in the $[\{\text{Sn}_3(\text{P}^i\text{Bu})_4\}_2(\text{K}\cdot\text{THF})_3]^-$ anion of **4**, it is interesting to note that the K⁺–K⁺ separation (4.033(2)–4.054(2) Å) is nonetheless shorter than expected for a van der Waals interaction (5.60 Å).³ It is also interesting to compare the structure of **4** with that of the Na analogue $[\{\text{Sn}_3(\text{P}^i\text{Bu})_4\}\text{Na}\cdot 3\text{THF}][\text{Na}(\text{THF})_5]^+$ (**3**). Although the latter is also ion separated, the coordination of only one Na⁺ cation in the $[\{\text{Sn}_3(\text{P}^i\text{Bu})_4\}\text{Na}\cdot 3\text{THF}]^-$ anion probably stems from a combination of the greater strength of Na–O bonds over K–O bonds and the greater size of K⁺ cations over Na⁺ cations. Thus, the structure of the $[\{\text{Sn}_3(\text{P}^i\text{Bu})_4\}_2(\text{K}\cdot\text{THF})_3]^-$ anion of **4** can be seen to arise essentially in order to minimize strain within the core, while the $[\{\text{Sn}_3(\text{P}^i\text{Bu})_4\}\text{Na}\cdot 3\text{THF}]^-$ anion of **3** can be seen to maximize solvation of the alkali-metal cations. The structure of the minor product $[\{\text{Sn}_4(\text{P}^i\text{Bu})_5\}\text{K}_2\cdot 5\text{THF}]$ (**5**) is that of a molecular (ion-paired) species in which a $[\text{Sn}_4(\text{P}^i\text{Bu})_5]^-$ anion coordinates two K⁺ cations (Figure 7), using a combination of shorter, terminal P–K (P(1a)–K(1) = 3.136(3) Å) and longer μ -P–K (P(3,4)–K(1) = 3.41 Å (mean)) bonds. In addition, the K⁺ cations are coordinated by terminal (range 2.69(1)–2.80(1) Å) and μ -O (2.759(7) Å) THF ligands. Thus, each of the K⁺ cations adopts a distorted-octahedral geometry (being bonded to three P atoms and three O atoms). Notably, this structural arrangement results in a K⁺–K⁺ separation in **5** (3.876(4) Å) even shorter than that found in **4**. Clearly, one factor making the

(14) For example, see: Klinkhammer, K. W. *Chem. Eur. J.* **1997**, *3*, 1418. Pu, L.; Haubrich, S. T.; Power, P. P. *J. Organomet. Chem.* **1999**, *582*, 100. Wiberg, N.; Wagner, H.-W.; Nöth, H.; Seifert, T. Z. *Naturforsch.* **1999**, *3*, 1418. Alvarez-Becedo, P.; Bond, A. D.; Haigh, R.; Hopkins, A. D.; Lawson, G. T.; McPartlin, M.; Moncrieff, D.; Mosquera, M. E. G.; Rawson, J. M.; Woods, A. D.; Wright, D. S. *Chem. Commun.* **2003**, 1288.

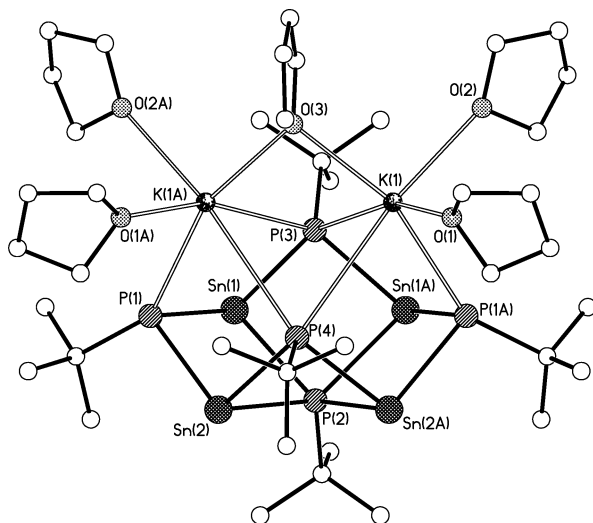
(15) For example, see: Beswick, M. A.; Bashall, A.; Hopkins, A. D.; Kidd, S. J.; Lawson, Y. G.; McPartlin, M.; Raithby, P. R.; Rothenberger, A.; Stalke, D.; Wright, D. S. *Chem. Commun.* **1999**, 739. Clegg, W.; Izod, K.; O'Shaughnessy, P. *Organometallics* **1999**, *18*, 2939. Rabe, G. W.; Heise, H.; Liable-Sands, L. M.; Guzei, I. A.; Rheingold, A. L. *Dalton Trans.* **2000**, 1863. Frenzel, C.; Somoza, F., Jr.; Blaurock, S.; Hey-Hawkins, E. *Chem. Commun.* **2001**, 3115.

(16) Beswick, M. A.; Choi, N.; Harmer, C. N.; Hopkins, A. D.; Paver, M. A.; McPartlin, M.; Raithby, P. R.; Steiner, A.; Tombul, M.; Wright, D. S. *Inorg. Chem.* **1998**, *37*, 2177.

Table 5. Selected Bond Lengths and Angles for $[\{\text{Sn}_3(\text{P}^t\text{Bu})_4\}_2(\text{K}\cdot\text{THF})_3]^-[\text{K}(\text{THF})_6]^+$ (4**)**

Bond Lengths (Å)			
Sn(1)–P(1)	2.609(2)	P(2)–K(1)	3.333(3)
Sn(1)–P(3)	2.609(2)	P(4)–K(1)	3.317(2)
Sn(1)–P(4)	2.614(2)	P(6)–K(1)	3.323(2)
Sn(2)–P(2)	2.604(2)	P(7)–K(1)	3.365(3)
Sn(2)–P(1)	2.620(2)	P(2)–K(2)	3.391(3)
Sn(2)–P(4)	2.613(2)	P(3)–K(2)	3.316(2)
Sn(3)–P(1)	2.588(2)	P(7)–K(2)	3.327(2)
Sn(3)–P(2)	2.623(2)	P(8)–K(2)	3.333(2)
Sn(3)–P(3)	2.615(2)	P(2)–K(3)	3.315(2)
Sn(4)–P(5)	2.613(2)	P(4)–K(3)	3.328(2)
Sn(4)–P(7)	2.610(2)	P(6)–K(3)	3.321(2)
Sn(4)–P(8)	2.608(2)	P(8)–K(3)	3.311(2)
Sn(5)–P(5)	2.608(2)	K(1,2,3)–O (in anion)	2.664(6) (mean)
Sn(5)–P(6)	2.612(2)	K(4)–O (in cation)	2.685(8)–2.777(8)
Sn(5)–P(8)	2.614(2)	K \cdots K (in anion)	4.033(2)–4.054(2)
Sn(6)–P(5)	2.592(2)		
Sn(6)–P(6)	2.616(2)		
Sn(6)–P(7)	2.616(2)		

Bond Angles (deg)			
P–Sn–P	83.99(6)–90.73(6)	P–K–P	65.78(5)–136.34(7)
Sn–P–Sn	94.60(6)–95.72(6)		

**Figure 7.** Structure of the heterometallic cages $[\{\text{Sn}_4(\text{P}^t\text{Bu})_5\}_2\text{K}_2\cdot 5\text{THF}]$ (**5**).

formation of either **4** or **5** possible in the 1:2 reaction of $\text{Sn}(\text{NMe}_2)_2$ with ${}^t\text{BuPHK}$ is the closeness of the stoichiometries of these complexes: i.e., in **4** a 4:3 ratio and in **5** a 5:4 ${}^t\text{BuP}:\text{Sn}$ ratio. However, the accessibility of either of these $\text{Sn}(\text{II})$ –phosphorus frameworks suggests that there is not at least an overwhelming difference between their thermodynamic stabilities. A possible explanation for this is that the advantage in adopting the structural arrangement of **5** is that it allows an overall increase in the coordination number of the K^+ cations; however, this is offset by an apparent increase in $\text{K}^+\cdots\text{K}^+$ repulsion and potentially an increase in cage strain compared to the arrangement found for **4**.

Closing Remarks

This paper has presented the first study of the effects of changing the alkali metal on the structures of the resulting family of heterometallic $\text{Sn}(\text{II})$ phosphinidene complexes, in the absence of the complication of P–P bond formation. One conclusion from this study is that the $\text{Sn}(\text{II})$ phosphinidene complex formed under these circumstances is strongly influenced by the coordination demands of the alkali metal present. The favored product in the case of Li^+ is the metallacyclic

Table 6. Selected Bond Lengths and Angles for $[\{\text{Sn}_4(\text{P}^t\text{Bu})_5\}_2\text{K}_2\cdot 5\text{THF}]$ (5**)^a**

Bond Lengths (Å)			
Sn(1)–P(1)	2.580(2)	P(1A)–K(1)	3.136(3)
Sn(1)–P(3)	2.609(2)	P(3)–K(1)	3.403(3)
Sn(1)–P(2)	2.703(2)	P(4)–K(1)	3.414(3)
Sn(2)–P(1)	2.574(2)	K(1) \cdots K(1A)	3.876(4)
Sn(2)–P(4)	2.603(2)	K–O terminal	2.69(1)–2.80(1)
Sn(2)–P(2)	2.726(2)	K– μ -O	2.759(7)

Bond Angles (deg)			
P(1)–Sn(1)–P(3)	96.89(7)	Sn(2)–P(1)–Sn(1)	87.23(7)
P(1)–Sn(1)–P(2)	95.52(8)	Sn(1)–P(2)–Sn(2)	81.83(5)
P(3)–Sn(1)–P(2)	82.74(7)	Sn(2A)–P(2)–Sn(2)	80.71(8)
P(1)–Sn(2)–P(4)	96.90(7)	Sn(1)–P(2)–Sn(1A)	81.91(8)
P(1)–Sn(2)–P(2)	95.08(8)	Sn(2)–P(2)–Sn(2a)	80.71(8)
P(4)–Sn(2)–P(2)	82.93(7)	Sn(1A)–P(3)–Sn(1)	85.54(9)
		Sn(2A)–P(4)–Sn(2)	85.45(9)

^a Symmetry transformation used to generate equivalent atoms: (A) $x, -y + 3/2, z$.

tetraanion $[\{\text{Sn}(\mu\text{-P}^t\text{Bu})_2(\mu\text{-P}^t\text{Bu})_2\}_2]^{4-}$. However, a switch to the $[\text{Sn}_3(\text{P}^t\text{Bu})_3]^-$ anion occurs when the size of the alkali metal is increased to Na and K. It is interesting to note that an overall 2:3 \rightarrow 3:4 \rightarrow 4:5 numerical progression is observed in the $\text{Sn}(\text{II})$: P^tBu ratios of the $[\{\text{Sn}_2(\text{P}^t\text{Bu})_3\}_2]^{4-}$, $[\{\text{Sn}_3(\text{P}^t\text{Bu})_4\}]^{2-}$, and $[\{\text{Sn}_4(\text{P}^t\text{Bu})_5\}]^{2-}$ anions of **1–3**, **4**, and **5** as the size of the alkali-metal cation is increased from Li^+ to Na^+ and then to K^+ . This suggests that the overall effect of increasing the size of the alkali metal to Rb^+ or Cs^+ may ultimately be to make the $[\text{Sn}_4(\text{P}^t\text{Bu})_5]^-$ anion favored over the $[\text{Sn}_3(\text{P}^t\text{Bu})_4]^-$ anion (since the $[\text{Sn}_4(\text{P}^t\text{Bu})_5]^-$ anion is likely to provide a better coordination environment for the larger alkali-metal cations). Unfortunately, we have not been able to test this hypothesis, since repeated attempts to obtain crystals from the 1:2 reactions of $\text{Sn}(\text{NMe}_2)_2$ with ${}^t\text{BuPHRb}$ or ${}^t\text{BuPHCs}$ failed, owing to the insolubility of products in a range of donor solvents.

Experimental Section

General Experimental Considerations. Compounds **1–5** are air- and moisture-sensitive. They were handled on a vacuum line (in an efficient cupboard) using standard inert-atmosphere techniques and under dry, oxygen-free argon.¹⁷ ${}^n\text{BuLi}$ in hexanes was obtained from Aldrich. PhCH_2M species ($\text{M} = \text{Na}, \text{K}$) were prepared from the reactions of ${}^t\text{BuOM}$ (Aldrich) with ${}^n\text{BuLi}$ in toluene.¹⁸ ${}^t\text{BuPH}_2$ was prepared by a modified version of the literature procedure.¹⁹ THF was dried by distillation over sodium/benzophenone prior to the reactions. PMDETA was distilled over Na metal and stored over molecular sieves under argon. The products were isolated and characterized with the aid of a nitrogen-filled glovebox fitted with a Belle Technology O_2 and H_2O internal recirculation system. Elemental analyses were performed by first sealing the samples under nitrogen in airtight aluminum boats (1–2 mg), and the C, H, and N content was analyzed using an Exeter Analytical CE-440 elemental analyzer. P analysis was obtained by spectrophotometric means. ${}^1\text{H}$, ${}^7\text{Li}$, and ${}^{31}\text{P}$ NMR spectra were recorded on a Bruker DPX 500 MHz spectrometer in dry d_8 -toluene (**1** only) or d_6 -benzene (**2–5**) (for ${}^1\text{H}$ NMR, using the solvent resonances as the internal reference standard) and d_8 -toluene (**1** only) or dry THF (**2–5**) (for ${}^{31}\text{P}$ NMR, using an acetone capillary to obtain a lock, referenced to an external standard of 85% H_3 -

(17) Shriver, D. F.; Drezdon, M. *The Manipulation of Air-Sensitive Compounds*, 2nd ed.; Wiley: New York, 1986.

(18) Hoffmann, D.; Bauer, W.; Hampel, F.; van Elkema Hommes, N. J. R.; Schleyer, P. v. R.; Otto, P.; Pieper, U.; Stalke, D.; Wright, D. S.; Snaith, R. *J. Am. Chem. Soc.* **1994**, *116*, 528.

(19) Kostyanovski, R. G.; El'natanov, Y. I.; Shikhaliev, S. M.; Ignatov, S. M. *Bull. Acad. Sci. USSR, Div. Chem. Sci.* **1982**, *31*, 1433.

$\text{PO}_4/\text{D}_2\text{O}$ and for ^{119}Sn NMR, using neat Me_4Sn as an external standard). ^7Li NMR spectra of **1** were recorded in d_8 -toluene and referenced to a saturated solution of $\text{LiCl}/\text{D}_2\text{O}$. The yields of all of the complexes are expressed in terms of the limiting amount of Sn supplied.

Synthesis of 1. To a solution of $^t\text{BuPH}_2$ (0.65 mL, 6.0 mmol) in toluene (20 mL) at -78°C was added $^n\text{BuLi}$ (4.1 mL, 6.6 mmol, 1.6 mol L^{-1} in hexanes). Stirring at room temperature (1 h) produced an orange precipitate of the monolithiate. To this suspension at -78°C was added a solution of $\text{Sn}(\text{NMe}_2)_2$ (0.42 g, 2.0 mmol) in toluene (10 mL). Warming to room temperature and stirring overnight led to the formation of an orange solution with some brown precipitate. The precipitate was filtered off (P3, Celite), and ca. 10 mL of solvent was removed under vacuum. Addition of THF (1.0 mL) to the orange solution, heating to ca. 60°C , and slow cooling to room temperature for 24 h gave orange single crystals of **1**. Yield: 0.25 g (38%, based on Sn supplied). ^1H NMR (25 $^\circ\text{C}$, 500.19 MHz, d_8 -toluene): δ 3.50 (m, 36H, THF), 1.51 (m, 36H, THF), 1.40 (s) (s, 54H, ^tBu). ^{31}P NMR (25 $^\circ\text{C}$, 161.975 MHz, d_8 -toluene): δ/ppm -184.9 (m, poorly resolved ^7Li -P coupling), 250.0 (m, poorly resolved ^7Li -P coupling). ^7Li NMR (25 $^\circ\text{C}$, 100.13 MHz, d_8 -toluene, relative to saturated $\text{LiCl}/\text{D}_2\text{O}$): δ/ppm 1.1 (s). No ^{119}Sn NMR signal could be found. Anal. Found: C, 35.2; H, 6.4. Calcd for **1**: C, 36.4; H, 6.5.

Synthesis of 2: To a solution of PhCH_2Na (0.57 g, 5.0 mmol) in THF (20 mL) at -78°C was added $^t\text{BuPH}_2$ (0.61 mL, 5.0 mmol), giving an orange-red solution. The solution was warmed to room temperature and heated to reflux for 20 min. The solution was then cooled to -78°C , and a solution of $\text{Sn}(\text{NMe}_2)_2$ (0.52 g, 2.5 mmol) in THF (10 mL) was added dropwise. The reaction mixture was warmed to room temperature and stirred overnight. The mixture was filtered (P3, Celite), and the solvent was removed in vacuo. The residue was recrystallized from THF (ca. 1.5 mL)/hexane (ca. 12.0 mL) at -20°C to yield orange crystals of **2**. Elemental analysis suggests that six THF molecules are removed by placing **2** under vacuum during isolation (10^{-1} atm, 15 min). Yield: 0.25 g (31%, based on Sn supplied). ^1H NMR (d_6 -benzene, 25 $^\circ\text{C}$, 500.2 MHz): δ 3.63 (m, $-\text{CH}_2\text{O}-$ THF), 2.17 (s, ^tBu), 1.46 (m, $-\text{CH}_2-$ THF). ^{31}P NMR (THF-acetone capillary, 25 $^\circ\text{C}$, 202.48 MHz): δ -145.2 (s, ca. 1P), 156.8 (s, minor), -175.9 (s, ca. 3P) (unresolved $^{119,117}\text{Sn}$ -satellites were observed for each of the resonances). ^{119}Sn NMR (THF-acetone capillary, 25 $^\circ\text{C}$, 186.68 MHz, relative to neat Me_4Sn): δ 803.0 (q, $J_{^{119}\text{Sn}-\text{P}} = 707.6$ Hz), 830.0 (br s, minor product). Anal. Found: C, 34.3; H, 6.5; P, 9.1. Calcd for **2**·6THF: C, 34.6; H, 6.2; P, 12.7.

Synthesis of 3. To a solution of PhCH_2Na (0.57 g, 5.0 mmol) in THF (20 mL) at -78°C was added $^t\text{BuPH}_2$ (0.61 mL, 5.0 mmol), giving an orange-red solution. The solution was warmed to room temperature and brought to reflux for 20 min. This solution was then cooled to -78°C , and a solution of $\text{Sn}(\text{NMe}_2)_2$ (0.52 g, 2.5 mmol) in THF (10 mL) was added dropwise. The reaction mixture was warmed to room temperature, stirred overnight, and then filtered through Celite. The solvent was removed in vacuo, and the product was dissolved in THF (2.0 mL), PMDETA (1.1 mL), and hexane (4.0 mL). Storage of the solution stored at -20°C yielded orange crystals of **3**. Yield: 0.28 g (28%, based on Sn supplied). ^1H NMR (d_6 -benzene, 25 $^\circ\text{C}$, 500.2 MHz): δ 2.31 (s, 36H, ^tBu), 2.24 (br s, PMDETA). ^{31}P NMR (THF-acetone capillary, 25 $^\circ\text{C}$, 202.48 MHz): δ -142.7 (s) (ca. 1P), -179.4 (ca. 3P) (unresolved $^{119,117}\text{Sn}$ satellites were observed for each of the resonances). ^{119}Sn NMR (THF-acetone capillary, 25 $^\circ\text{C}$, 186.68 MHz, relative to neat Me_4Sn): δ 802.8 (q, $J_{^{119}\text{Sn}-\text{P}} = 704$ Hz), 757.3 (br s, minor component). Anal. Found: C, 39.1; H, 7.7; N, 7.2; P, 9.8. Calcd for **3**: C, 38.9; H, 7.7; N, 6.9; P, 10.6.

Synthesis of 4/5. The synthetic procedure and scale were identical with those used for **2**, only using PhCH_2K (0.66 g, 5 mmol) instead of PhCH_2Na . The products were again crystallized from

hexane/THF. Generally, only yellow needles of **4** were obtained. However, on occasions up to ca. 5% of **5** (orange hexagons) also crystallized along with **4**. Yield: 0.23 g (24%, based on Sn supplied and assuming only **4** is formed). ^1H NMR (d_6 -benzene, 25 $^\circ\text{C}$, 500.2 MHz): δ 3.68 (m, $-\text{CH}_2\text{O}-$ THF), 2.17 (br s, ^tBu), 1.51 (m, $-\text{CH}_2-$ THF). ^{31}P NMR (THF-acetone capillary, 25 $^\circ\text{C}$, 202.48 MHz): δ very broad resonances at -123.2 (s), -135.2 (s), -143.0 (s), -153.3 (s) (major). ^{119}Sn NMR (THF-acetone capillary, 25 $^\circ\text{C}$, 186.68 MHz, relative to neat Me_4Sn): δ 846.0 (very br s). Anal. Found: C, 31.6; H, 6.1; P, 11.3. Calcd for **4**: C, 36.2; H, 6.4; P, 11.0. Calcd for **4**·4THF: C, 32.3; H, 5.8; P, 12.8.

Crystallographic Studies of 1–5. Crystals of **1**, **2**, **3**·0.5-(hexane), **4**·THF, and **5**·2THF were mounted directly from solution under argon using an inert oil, which protected them from atmospheric oxygen and moisture.²¹ X-ray intensity data were collected using a Nonius Kappa CCD diffractometer. Details of the data collections and structural refinements are given in Table 1. For all of the crystals the positions of the non-hydrogen atoms were located by direct methods and refinement was based on F^2 .²⁰ In the crystals of compound **2** the Na(1) and P(1) atoms are on one C_3 axis and Na(2) on a second, so that both cation and anion have crystallographic 3-fold symmetry. The middles of the molecules of **1** lie on a crystallographic inversion center, so that overall the molecules are centrosymmetric. The molecules of **5** and two THF solvate molecules are bisected by a crystallographic mirror plane, and one THF ligand lies in the plane. Relatively high atomic displacement parameters for carbon atoms in all five compounds indicated some conformational or rotational disorder of the peripheral groups. Many of the THF molecules were resolved into two components, including two independent THF ligands in **1** (70:30 and 60:40), three independent THF molecules in **2** (all 50:50), the THF ligand in **3** (50:50), three THF ligands in the anion of **4** (two 50:50 and one 70:30), and two independent THF ligands remote from the mirror plane in **5** (both 50:50). The three independent ^tBu groups in **1** were each resolved into two components (two 60:40 and one 70:30). The PMDETA ligand in **3** was resolved with difficulty into equal overlapping components related by a rotation of ca. 60° round the pseudo- C_3 axis of the Sn_4P_4 core. Residual electron density in the lattice of **3** was assigned to a half n -hexane solvate molecule. Due to relatively poor diffraction at high angles, attributable to the disorder, data in a limited θ range ($<21^\circ$) was used in the refinement of **5**. In the final cycles of full-matrix least-squares refinement, anisotropic displacement parameters were assigned to the full occupancy non-hydrogen atoms in all five structures. The hydrogen atoms for all five structures were placed in calculated positions with displacement parameters set equal to $1.2U_{\text{eq}}$ (or $1.5U_{\text{eq}}$ for methyl groups) of the parent carbon atoms.

Acknowledgment. We thank the EPSRC (M.M., C.M.P., A.R., D.S.W.), The Cambridge European Trust and Newton Trust (F.G.), The States of Guernsey and The Domestic and Millennium Fund (R.A.K.), The EU (Erasmus grant for J.P.H.), and The Konrad-Adenauer-Stiftung (J.P.H.) for financial support. Acknowledgment is made to the donors of the Petroleum Research Fund, administered by the American Chemical Society, for partial support of this research (M.L.S.).

Supporting Information Available: CIF files and figures giving full listings of X-ray crystallographic data, atomic coordinates, thermal parameters, bond distances, bond angles, and hydrogen parameters and Ortep plots for **1–5**. This material is available free of charge via the Internet at <http://pubs.acs.org>.

OM060167M

(20) Kottke, T.; Stalke, D. *J. Appl. Crystallogr.* **1993**, *26*, 615.

(21) Sheldrick, G. M. SHELX-97; University of Göttingen, Göttingen, Germany, 1997.